O81

Na^+,K^+-ATPase subunit isoforms in rat dorsal root ganglia of the regenerating sciatic nerve

M.F. Arteaga*, R. Gutierrez†, J. Avila*, L. Díaz-Flores† and P. Martín-Vasallo*

*Departments of *Bioquímica y Biología Molecular and †Anatomía Patológica, Universidad de La Laguna. Avda Astrofísico Sánchez s/n, 38206 La Laguna, Tenerife, Spain*

The Na^+,K^+-ATPase is the membrane bound enzyme that maintains the K^+ and Na^+ intracellular gradients used in the nervous system (NS) by other proteins for electrical membrane potential changes and uptake of neurotransmitters. In astrocytes, it participates in the uptake of K^+ after depolarization of neurons. The system consists of two subunits: the α subunit (112 kDa) and the β subunit (a 45 kDa glycoprotein). The α has four different isoforms. In brain, $\alpha 2$ predominates in astrocytes and $\alpha 3$ in neurons, and $\alpha 1$ is ubiquitous. The β subunit has also four different isoforms. $\beta 3$ in the NS is only expressed in photoreceptors and oligodendrocytes. All $\alpha\beta$ combinations may exist and the patterns of subcellular and developmental specification are extremely complex. Also control of biosynthesis and the enzyme properties, such as ion affinities, are affected by the choice of α and β. The aim of this study was to determine the cellular redistribution of Na^+,K^+-ATPase subunit isoforms after injury of the sciatic nerve of the rat. We performed double-labelling (ATPase/cell-specific markers) immunofluorescence in frozen sections of dorsal root ganglia (DRG) of the regenerating tissue using isoform-specific antibodies. Samples were collected from Sprague-Dawley rats after sciatic nerve transection and reconstruction into a Silastic chamber 1.47 mm diameter under ketamine anaesthesia, in both cases: during surgery and during sample collecting. Once samples were collected, animals were killed by overdosage of anaesthesic.

We have found that $\alpha 1$ and $\alpha 2$ immunoreactivities in normal DRG are similar in intensity and localization in the plasma membrane of all kinds of cells, with no signal for $\alpha 3$ isoform. After injury $\alpha 1$ and $\alpha 2$ expression decreases evenly in all cells and there is a remarkable onset in the expression of $\alpha 3$, with a peak about day three and it gradually disappears during regeneration.

Regarding β subunits isoforms, $\beta 1$ immunoreactivity is restricted to a perinuclear halo of neurons, with no dependence on the kind or shape of neurons, and to the cytoplasm of the small glial cells surrounding these neurons. No $\beta 2$ was found. $\beta 3$ specific immunofluorescence is most abundant in the cytoplasm of small neurons and much less abundant in big and medium size neurons.

Suddenly after injury, $\beta 1$ shows a homogeneous distribution in the soma of neurons. As regeneration proceeds, this isoform recovers its original emplacement around the nucleus, although a faint signal still remains all over the cytosol.

The $\beta 3$-specific immunolabelling signal in small neurons progressively decays after injury until day 3, then the signal increases in intensity, becoming stronger than previous to injury at day 7 then progressively decreases to normal levels.

The diversity of Na^+,K^+-ATPase subunit isoforms and their complex cellular, spatial and temporal patterns of cellular expression in the DRG suggest that Na^+,K^+-ATPase isozymes perform specialized physiological functions during regeneration.

All procedures accord with current National and local guidelines.

O82

Changes in Na^+ distribution across the crypt wall in isolated rat distal colon during transition from high to low NaCl diets

Richard J. Naftalin *, Iram Afzal, Concepció Amat, Anna Pérez-Bosque and Miquel Moretó

*Departments of Physiology, Facultat de Farmacia, Universitat de Barcelona, Spain and *King's College London, Guy's Campus, London, UK*

Rat descending colon absorbs fluid and Na^+ against a high luminal hydraulic resistance and absorption is increased by a reduction in Na^+ intake (Naftalin *et al.* 1999). We have now investigated whether the effects of low Na^+ (LS) diet are due to increased osmotic concentration gradients, generated by Na^+ and reduced solute leakage across the crypt wall.

Experiments were conducted on Sprague-Dawley rats (200–250 g) that were fed a high NaCl (HS) diet (NaCl 4500 μmol day^{-1}) for 8–9 days and then switched to a LS diet (NaCl 35 μmol day^{-1}) ± captopril (125 mg kg^{-1} day^{-1}) for 1–9 days then were humanely killed prior to tissue isolation. Experiments were approved by the Ethical Committee in Animal Experimentation of the University of Barcelona.

$[Na^+]$ in isolated rat distal colonic mucosa from rats was determined using a modification of a dual wavelength laser scanning confocal microscopic method in which low affinity Na^+-sensitive dye (Sodium Red, and BODIPY) is bound to 50 nm diameter polystyrene beads (Jayaraman *et al.* 2001). Crypt permeability to dextran was monitored by the rate of escape of FITC labelled dextran (10 kDa) from the crypt lumen into the pericryptal space at 37°C. These effects were correlated with plasma aldosterone and with trophic changes in crypt colonocytes, pericryptal myofibroblasts and the surrounding extracellular matrix, using immunolocalization in paraformaldehyde-fixed colon, with specific antibodies and fluorescence-labelled secondary antibodies. The $[Na^+]$ in the pericryptal sheath of HS rats was 144 ± 4 mM ($n = 4$; S.E.M.), and in the crypt lumen 5–10 μm distal to the opening $[Na^+]$ fell to 75–65 mM. During 9 days after switching to LS diet, pericryptal $[Na^+]$ increased, to 285 ± 7 mM (S.E.M.) ($n = 5$, $P < 0.025$ Students unpaired *t* test) as in murine distal colonic crypts *in vivo* (Thiagarajah *et al.* 2001), but luminal $[Na^+]$ was unaltered. Recovery of pericryptal $[Na^+]$ 3–5 days after switching to LS diet was significantly delayed in captopril-treated rats. Crypt wall permeability to dextran decreased by 4–5-fold within 3 days but was delayed by captopril. Significant captopril-sensitive increases in the pericryptal myofibroblast smooth muscle actin, OB-cadherin, collagen IV expression and also increases in ATII type I and TGF-β receptors within 3 days after switching to LS diet.

Jayaraman S *et al.* (2001). *J Clin Invest* **107**, 317–324..

Naftalin RJ *et al.* (1999). *J Physiol* **515**, 201–210.

Thiagarajah J *et al.* (2001). *Am J Physiol* **281**, C1898–C1903.

This work was supported by The Wellcome Trust

All procedures accord with current National and local guidelines.

O83

Cellular localisation of natural cystathionine-β-synthase domain mutants of CLC-5 investigated using N-terminal GFP–mCLC-5 fusion proteins

G. Carr, J.A. Sayer and N.L. Simmons

School of Biosciences, Medical School, Framlington Place, University of Newcastle upon Tyne, NE2 4HH, UK

The Cl^- channel, CLC-5, associated with Dent's disease in humans consists of 746 amino-acids with intracellular N and C terminals. Two cystathionine-β-synthase (CBS) domains are present at the C-terminal and are thought to be necessary for correct trafficking of the CLC-5 protein or for correct channel function (Jentsch *et al.* 2002). Three natural mutations of CLC-5 (R648X, R704X and the frameshift mutation 695delCfs) give rise to Dent's disease in humans by affecting CBS domain 2.

We used site-directed mutagenesis to prepare the R648X, R704X and 695delCfs mutants of mCLC-5 contained in the mammalian expression vector pcDNA3.1-NT–GFP. The mouse mCLC-5 is 97 % identical to the human protein at the amino acid level, with virtual identity at the C-terminal (excepting for a conservative L699M difference). We then compared the cellular distributions of N-terminal GFP–mCLC-5 mutant proteins and wild-type after transient transfection of CHO-K1 and mIMCD-3 cells and imaging of positive transfectants by confocal laser scanning microscopy. Post transfection, unfixed cells were pre-incubated with TRITC-wheat germ lectin (50 μg ml^{-1}) for 2 min or 1 h.

In CHO-K1 cells transient transfection of wild-type mCLC-5 is associated with the appearance of a characteristic strongly outwardly rectifying DIDS-insensitive Cl^- conductance (Sayer *et al.* 2001). WT-mCLC-5-NT–GFP colocalises with plasma membrane TRITC-WGA (2 min incubation) as well as being present within endosomes. The R648X, R704X and 695delCfs mutants of mCLC-5 all show an altered distribution, being absent from the plasma membrane whilst being retained at a perinuclear localisation. In mIMCD-3 cells, plasma membrane expression of WT-mCLC-5-NT-GFP is absent, expression being entirely intracellular. The R648X, R704X and 695delCfs mutants of mCLC-5 are again retained at a perinuclear localisation. Furthermore, expression of CBS mutant proteins together with treatment of mIMCD-3 cells with TRITC-WGA (1 h) shows restricted endocytic uptake of the lectin.

We conclude that CBS-2 is associated with the direction of trafficking of mCLC-5. Failure to measure Cl^- currents with CBS mutants (Lloyd *et al.* 1996) may be associated with a failure of protein traffic to the plasma membrane as is seen in CHO-K1 cells.

Jentsch TJ *et al.* (2002). *Physiol Rev* **82**, 503–568.

Lloyd SE *et al.* (1996). *Nature* **379**, 445–449.

Sayer JA *et al.* (2001). *J Physiol* **536**, 769–783.

This work was supported by the NKRF.

O86

Bidirectional solute and fluid flows and driving forces unravelled in cultured bovine tracheal epithelium

S. Jalickee*, J.W. Widdicombe‡, S.S. Miller*† and S. Tripathi*§

**School of Optometry and †Department of Molecular and Cell Biology, University of California, Berkeley, CA, USA, ‡University of California, Davis, CA, USA and §Tata Institute of Fundamental Research, Mumbai, India*

The forces, molecular mechanisms, and solute gradients which drive bidirectional solute-coupled water transport across epithelia have not been unequivocally described, let alone quantified. We report high-resolution transepithelial volume flow measurements across primary cultures of bovine tracheal epithelial cells on permeable supports in experiments designed to (1) estimate the driving forces for fluid absorption/secretion, (2) test correlation of net volume flux with the calculated short-circuit current, and (3) test the effects of counterion transport number on net solute flow under symmetric conditions.

Bovine tracheal epithelial cells obtained from abattoir material were grown to confluence in primary culture on permeable filters (Costar 3401) as described (Kondo *et al.* 1993). Filters (0.5 cm^2) were mounted in mammalian Ringer solution at 36 °C in a Kel-F chamber (Jiang *et al.* 1993) for simultaneous measurement of transepithelial volume flow with a capacitance probe and transepithelial potential and resistance. The entire experiment was done with high precision control of ambient parameters, particularly temperature. By layering the meniscus of each hemichamber with hexadecane, background volume losses were totally eliminated and the capacitance probe tracked transepithelial volume flow with high stability. Student's paired *t* test was used to calculate significance.

Serosal ouabain (> 10 μM) abolished absorption (from 17.2 ± 1.1 to −1.1 ± 2.6 $\mu l\ cm^{-2}\ h^{-1}$ (S.D.; $n = 2$) as did 10 μM apical amiloride (from 14.0 ± 3.9 to 0.6 ± 2.4 $\mu l\ cm^{-2}\ h^{-1}$ (S.E.M.; $n = 10$, $P < 0.001$). Simultaneous bilateral substitution of Cl with gluconate changed spontaneous absorption from 5.2 ± 1.0 $\mu l\ cm^{-2}\ h^{-1}$ to a secretion of 0.8 ± 2.6 $\mu l\ cm^{-2}\ h^{-1}$ (S.E.M.; $n = 4$, $P < 0.05$) without a significant change in the calculated short-circuit current. Serosal hyperosmolarity (sucrose 20–25 mmol, normalised to 20 mmol) in either Cl^--containing or Cl^--free solutions increased absorptive flow from 4.0 ± 2.8 to 18.4 ± 2.4 $\mu l\ cm^{-2}\ h^{-1}$ (S.E.M.; $n = 10$, $P < 0.001$).

We conclude that (1) absorptive flows are generated osmotically by Na^+ absorption with gradients of the order of 20 mmol, (2) a Cl^--independent secretory flow exists which is not accounted for electrically, and (3) this epithelium is a useful model for both fluid absorption and secretion.

Jiang C *et al.* (1993). *Science* **262**, 424–427.

Kondo M *et al.* (1993). *In Vitro* **29A**, 19–24.

This work was supported by NIH and MIBRS.

All procedures accord with current National and local guidelines.

O87

A Na^+-selective, apical conductance in dexamethasone-treated H441 human bronchial epithelial cells

S.J. Ramminger, K. Richard, R.E. Olver and S.M. Wilson

Lung Membrane Transport Group, Tayside Institute of Child Health, Department of Maternal and Child Health Sciences, Ninewells Hospital and Medical School, University of Dundee, Dundee DD1 9SY, UK

Dexamethasone-treated H441 bronchial epithelial cells spontaneously generate amiloride-sensitive I_{SC} attributable to expression of the epithelial Na^+ channel subunits (α-, β-and γ-ENaC) and a consequential rise in amiloride-sensitive apical conductance (G_{amil}) (Sayegh *et al.* 1999). However, these subunits can form a range of Na^+ channel isoforms that differ in their relative conductances to Na^+ and K^+ (Jain *et al.* 2001). It is therefore impossible to infer the conductive properties of the channels underlying this response and so we now explore the conductive properties of the apical membrane in dexamethasone-treated H441 cells.

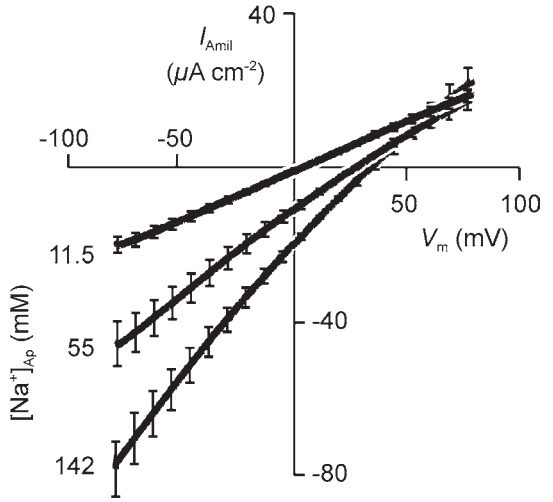

Figure 1. Apical membrane currents in dexamethasone-treated cells. Cultured epithelia were bathed symmetrically with a cytoplasm-like solution ($[Na^+]$ = 11.5 mM, $[K^+]$ = 135.3 mM) and permeabilised with nystatin (75 μM) and ouabain (1 mM). The figure shows the current–voltage relationship (means ± S.E.M., values of V_m were corrected for changes in liquid junction potential) for the amiloride-sensitive component of the apical membrane current recorded under symmetrical conditions and in the presence of inwardly directed Na^+ gradients.

Under hormone-free conditions only ~50 % of cultures formed resistive epithelia (344 ± 86 Ω cm^2, mean ± S.E.M.) and these generated very little I_{SC} (1.3 ± 0.6 μA cm^{-2}). However, dexamethsaone-treated (0.2 μM) cells consistently grew into coherent epithelial sheets (586 ± 47 Ω cm^2) that generated substantial currents (21.5 ± 2.3 μA cm^{-2}) (see also Sayegh *et al.* 1999). This hormone had no effect upon the current due to Na^+ pump activity (control: 40.8 ± 7.8 μAcm^{-2}; dexamethasone-treated: 34.3 ± 3.8 μAcm^{-2}), which was estimated as described by Baines *et al.* (2001), and so this response must reflect an effect on the apical membrane. Examination of apical membrane currents showed that inwardly directed Na^+ gradients caused a rightward shift in V_{rev} (Fig. 1) and analysis of these data indicated that G_{amil} was 4.2-fold more permeable to Na^+ than to K^+. The increase in I_{SC} can thus be attributed to the induction of a selective, apical Na^+ conductance.

Baines DL *et al.* (2001). *J Physiol* **532**, 105–113.

Jain L *et al.* (2001). *Am J Physiol Lung Cell Mol Physiol* **280**, L646–L658.

Sayegh R *et al.* (1999). *J Biol Chem* **274**, 12431–12437.

This work was supported by the Wellcome Trust.

O88

Pharmacologically distinct, basolateral P2Y receptors for ADP and UTP in Calu-3 human airway epithelial cells

M.T. Clunes, R.E. Olver and S.M. Wilson

Lung Membrane Transport Group, Tayside Institute of Child Health, Department of Maternal and Child Health Sciences, Ninewells Hospital and Medical School, University of Dundee, Dundee DD1 9SY, UK

Calu-3 cells respond to basolateral nucleotides with increases in intracellular free calcium ($[Ca^{2+}]_i$) (Clunes *et al.* 2002). In the present study, we have characterised the receptors underlying these responses in Fura-2-loaded Calu-3 cells grown (2–4 days) on collagen-coated permeable supports (Costar, Transwell Col). Supports were mounted in a specialised chamber, which allowed independent perfusion of the apical and basolateral surfaces (2–3 ml min^{-1}), and attached to the stage of an inverted microscope equipped with extra long working distance optics. The Ca^{2+} signals evoked by pulses of basolateral nucleotides were quantified (as arbitrary units, means ± S.E.M.) by integrating the increase in Fura-2 fluorescence ratio with respect to time.

Initial experiments confirmed (Clunes *et al.* 2002) that ATP (EC_{50} 10.6 ± 1.67 μM, maximal response at 100 μM, n = 6), ADP (EC_{50} 3.5 ± 0.3 μM, maximal response at 100 μM, n = 5) and UTP (EC_{50} 53.7 ± 5.6 μM, maximal response at 300 μM, n = 6) all evoked rapid increases in $[Ca^{2+}]_i$. In further experiments cells were exposed to a series of five pulses (30 s) of agonist, delivered at 2 min intervals, in order to evoke autologous desensitisation (> 85 %) to particular nucleotides. We then explored the extent to which these desensitised cells retained sensitivity to other nucleotides. UTP-desensitised cells (300 μM) displayed responses to ADP (100 μM) that were similar to control and ADP-desensitised (100 μM) responded normally to 300 μM UTP (5.86 ± 1.70 arbitrary units). In contrast, the response to ATP was smaller than normal in both groups of cells ($P < 0.05$ for both, Student's unpaired t test). Further experiments showed that suramin (10 μM) had no effect upon the concentration–effect curves for UTP (control: EC_{50} = 30 ± 3 μM, threshold 3 μM, n = 4; suramin-treated: EC_{50} = 47 ± 4 μM, threshold 3 μM, n = 3) but shifted the curve for ADP to the right (control: EC_{50} = 0.88 ± 0.33 μM, threshold 30 nM, n = 4; suramin-treated EC_{50} = 19.4 ± 0.3 μM, threshold 3 μM, n = 6).

ATP thus activates a complex receptor population but UTP and ADP seen to be selective agonists for different receptor subpopulations that can be distinguished on the basis of their sensitivity to suramin. The high affinity for ADP and the sensitivity to suramin suggest that one of these subpopulations corresponds to the well-documented $P2Y_1$ receptor, but further studies are needed to identify the receptor population that can be activated by UTP but which is insensitive to suramin.

Clunes MT *et al.* (2002). *J Physiol* **544.P**, 97*P*.

This work was supported by the Wellcome Trust and Tenovus Scotland.

O89

Na^+,K^+-ATPase is down-regulated in canine prostate cancer

I. Evans*, R.V. Floyd*, R. Fox†, C.S. Foster‡, P. Martín-Vasallo§ and A. Mobasheri*

*Departments of *Veterinary Preclinical Sciences, †Veterinary Pathology and ‡Cellular and Molecular Pathology, University of Liverpool, Liverpool L69 3BX, UK and §Laboratorio de Biologia del Desarrollo, Departamento de Bioquimica y Biologia Molecular, Universidad de La Laguna, 38201 La Laguna, Tenerife, Spain*

The principal physiological function of the prostate gland is the synthesis, accumulation and secretion of citrate. In prostate cancer, citrate production levels are significantly reduced as a result of the altered cellular metabolism and bioenergetics (Costello & Franklin, 1997, 2000). Na^+,K^+-ATPase function is essential for citrate production since the inward Na^+ gradients generated by Na^+,K^+-ATPase are utilized for the Na^+-dependent uptake of aspartate, a major substrate for citrate synthesis. Accordingly, the objective of this study was to compare the localization and relative abundance of Na^+,K^+-ATPase isoforms in normal dog prostate, benign prostatic hyperplasia (BPH) and prostatic adenocarcinoma (PCa) in order to see if reduced citrate levels in PCa are accompanied by changes in Na^+,K^+-ATPase expression.

Dog prostate glands were obtained from animals humanely killed for clinical reasons. Prostates were fixed in formaldehyde and embedded in paraffin before sectioning and immunohistochemical staining using a panel of well-characterized monoclonal and polyclonal antibodies raised against known Na^+,K^+-ATPase subunit isoforms.

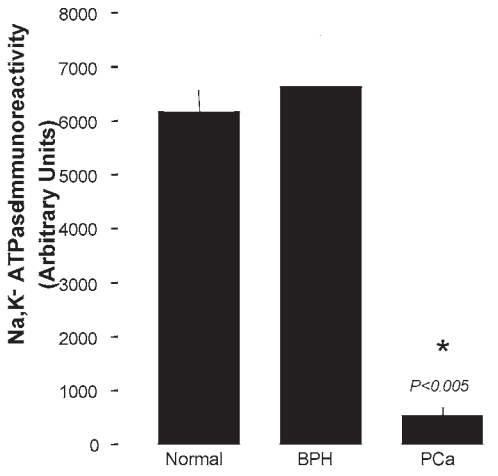

Figure 1. Quantitative analysis of Na^+,K^+-ATPase immunoreactivity in normal, BPH, and PCa canine prostate. Data are presented as means ± S.E.M., $n = 3$ in each independent group. *Data were compared with Student's t test.

Expression of Na^+,K^+-ATPase $\alpha1$, $\beta1$ and $\beta2$ and, was observed in the lateral and basolateral plasma membrane domains of prostatic epithelial cells in normal and BPH prostates. We did not detect the γ subunit of Na^+,K^+-ATPase in any of the normal, BPH or PCa tissues examined. The $\alpha1$ isoform was detected in abundance but there was no evidence of $\alpha2$ or $\alpha3$ isoform expression in prostatic epithelial cells. In advanced PCa prostates Na^+,K^+-ATPase isoform expression was reduced by more than 90 % compared to normal and BPH glands (Fig. 1). Dog prostate Na^+,K^+-ATPase consisted primarily of $\alpha1/\beta1$ and $\alpha1/\beta2$ isoenzymes. These isoform proteins were predominantly localized to the basolateral plasma membrane domains of prostatic epithelial cells in normal and BPH specimens. The abundant basolateral immunostaining observed in normal and BPH glands was significantly attenuated in PCa sections as revealed by image analysis. The metabolic transformation of zinc-accumulating citrate-producing normal prostate epithelial cells to citrate-oxidizing malignant cells has important implications for cellular bioenergetics, and metabolism and appears to be accompanied by a down-regulation of Na^+,K^+-ATPase.

Costello LC & Franklin RB (1997). *Urology* **50**, 3–12.

Costello LC & Franklin RB (2000). *Oncology* **59**, 269–282.

This study was supported by a grant from the Pet Plan Charitable Trust (UK).

All procedures accord with current UK legislation.

O90

Developmental changes in L-carnitine and creatine transport in rat kidney

M. García-Delgado, J.M. Durán, M.J. Peral, M.L. Calonge and A. Ilundáin

Departamento de Fisiología y Zoología, Facultad de Farmacia, Universidad de Sevilla, 41012-Sevilla, Spain

L-Carnitine and creatine transporters, OCTN2 and CRT1, respectively, are located on the apical membrane of renal tubular epithelial cells. They are important for the concentrative reabsorption of L-carnitine and creatine, respectively, after their glomerular filtration in the kidney. In the current work, the ontogeny of L-carnitine and creatine transport by rat renal brush border membrane (BBM) has been studied.

BBM Vesicles (BBMV) were isolated from the kidney of newborn (1 day postpartum), suckling (16–18 days), weaning (30 days) and adult (2- and 7-month-old) Wistar rats. The animals were terminally anaesthetized with ether and humanely killed. BBMV were obtained using the method of Biber *et al.* (1981). L-[^{14}C]carnitine or [^{14}C]creatine uptake into BBMV was measured by a rapid filtration technique.

It was observed that BBMV of newborn Wistar rats transport L-carnitine and creatine and that the rate of transport of the two solutes increased with age, reaching a plateau at 1 month old. Kinetic studies revealed that the maximal rate of transport, V_{max}, increased with development from 6.4 ± 0.2 at 1 day old ($n = 3$) to 42.1 ± 2.4 at 2 months old ($n = 3$) for creatine, and from 0.8 ± 0.03 at 1 day old ($n = 2$) to 4.0 ± 0.08 at 1 month old ($n = 8$) for L-carnitine. However, no changes in K_m values (12 μM ($n = 16$) for creatine and 48 μM ($n = 12$) for L-carnitine) were observed. These observations suggest an increase in either the density or the turnover of transporters during ontogeny. Northern blot analysis revealed one transcript for OCTN2 of 3.7 kb and two for CRT1 of 3.2 kb and 4.9 kb. In all cases, the intensity of the bands were low at birth and increased throughout development, approaching maximum levels at 30 days of age.

In conclusion, transport activity and mRNA expression levels of L-carnitine and creatine are increased with age.

Biber J *et al.* (1981). *Biochim Biophys Acta* **647**, 169–176.

This work was supported by a grant from the Spanish Ministerio de Ciencia y Tecnología (DGICYT PM99-0121).

All procedures accord with current National and local guidelines.

P32

Ethanol increases renal AQP2 expression in adult rats and their offspring

Marta García-Delgado, María J. Peral, Olga García-Benítez, Olimpia Carreras and Anunciación A. Ilundáin

Departamento Fisiología y Zoología, Facultad de Farmacia, Universidad de Sevilla, 41012 Sevilla, Spain

Studies on renal water excretion were carried out in suckling Wistar rats born to mothers given ethanol (Tavares *et al.* 1999) during gestation and the suckling period and the results were compared to offspring of dams given diets containing no ethanol. Comparisons were also made between progenitors (mothers and fathers) with or without prolonged ethanol ingestion.

The experiments were performed in accordance with the requirements of the European convention for the care and use of laboratory animals. Rats were anaesthetized by I.P. injection of urethane (14 %). Plasma levels of arginine vasopressin (AVP) and aldosterone, urine and renal papillary osmolality, urine outflow and kidney aquoporin 2 (AQP2) expression were determined (Murillo-Carretero *et al.* 1999; Peral *et al.* 2002). For urine collection, metabolic cages were used. Apical membranes were isolated as previously described (Garcia-Delgado *et al.* 2001).

Maternal ethanol ingestion during pregnancy and the suckling period decreases urine outflow and increases urine and renal papillary osmolality of the offspring. These changes were also observed in the ethanol-treated progenitors, although they were of smaller magnitude. In the offspring, ethanol exposure increases kidney AQP2 mRNA expression and apical membrane protein abundance by 1.5- and 3-fold, respectively. In the case of the progenitors, ethanol treatment increases renal AQP2 mRNA expression and apical membrane protein abundance 2- and 1.5-fold, respectively. Plasma levels of AVP and aldosterone tend to increase in the ethanol-exposed animals, but the increases were not significant.

These results suggest that the ethanol-related decrease in urine outflow is associated with up-regulation of AQP2 expression, which appears to be independent of plasma levels of either AVP or aldosterone.

Garcia-Delgado M *et al.* (2001). *J Am Soc Nephrol* **12**, 1819–1825.

Murillo-Carretero MI *et al.* (1999). *J Am Soc Nephrol* **10**, 696–703.

Peral MJ *et al.* (2002). *J Physiol* **545**, 133–144.

Tavares E *et al.* (1999). *Life Sci* **64**, 2001–2010.

This work was supported by grants from the Spanish DGICYT PM99-0121 and PM98-159.

All procedures accord with current National and local guidelines.

P33

D-Mannose transport in isolated enterocytes: evidence for a Na^+-independent, D-mannose-specific transporter

Juan M. Durán, Mercedes Cano and Anunciación A. Ilundáin

Departamento Fisiología y Biología Animal, Facultad de Farmacia, Universidad de Sevilla, 41012 Sevilla, Spain

We have previously shown that the apical membrane of chicken small intestine has a Na^+–D-mannose cotransport system (Cano *et al.* 2001). In the current study D-[^{14}C]mannose transport has been studied in enterocytes isolated from Hubbard chickens, 4–6 weeks old. The animals were killed by decapitation. The results show that following incubation in the presence of Na^+, part of the D-mannose taken up by the cells is either metabolized (phosphorylated or bound to membrane components) or remains in a readily diffusive form. The nature of the cytosolic radioactivity was determined by ethanol–water extraction of the cells. Thin layer chromatography of the extracts revealed a peak ($R_f = 0.8$), which accounts for 80 % of the total applied radioactivity and migrates with free D-mannose, and another peak ($R_f = 0.1$) that migrates with the phosphorylated mannose. The cytosolic mannose that remains as a readily diffusive form is released from the cells by either adding cold D-mannose or transferring the cells into an ice bath. Following 30 min mannose uptake in the presence of Na^+, the addition of either phloretin or cytochalasin B (inhibitors of Glut2 transporter) slightly reduced the previously accumulated D-mannose. These two agents, however, increased the cell to external medium 3-oxymethyl-glucose concentration ratio. D-Mannose efflux rate from preloaded D-[^{14}C]mannose enterocytes is Na^+ independent and insensitive to phloretin and cytochalasin B. It is concluded that part of the mannose taken up by the enterocytes is metabolized and that enterocytes have two D-mannose transport systems: one is concentrative and Na^+ dependent and the other is Na^+ independent, passive and different from Glut2.

Cano M *et al.* (2001). *Pflugers Archiv* **441**, 686–669.

This work was supported by grants from the Spanish DGICYT PM99-0121.

All procedures accord with current National and local guidelines.

P34

GLUT8 expression in mouse intestine: identification of several transcripts

A. Romero and J.E. Mesonero

Physiology, Health and Experimental Sciences Faculty, Cardenal Herrera-CEU Univesity, 46113-Moncada (Valencia), Spain

GLUT8 is a novel glucose transporter that exhibits significant sequence similarity with the members of the sugar transport facilitator family GLUT. This novel glucose transporter was independently cloned by several research groups (Doege *et al.* 2000; Ibberson *et al.* 2000; Carayannopoulos *et al.* 2002). Human and mouse sequences have 86.2 % identical amino acids and comprise twelve putative membrane-spanning helices and several conserved motifs. GLUT8 is expressed to some extent in insulin-sensitive tissues, e.g. heart, skeletal muscle and adipose tissue. However, the highest levels of GLUT8 mRNA were found in testis and appeared to be hormonally regulated. GLUT8 is also expressed in the small intestine, where the glucose transport is modulated by hormones.

The purpose of the present study was to examine GLUT8 expression in mouse enterocytes and compare this with other tissues, in an attempt to determine GLUT8 contribution to intestinal glucose absorption.

Handling, equipment used, and killing of mice was carried out in accordance with the European Council legislation 86/609/EEC concerning experimental animal protection. After killing, tissues (jejunum, colon, kidney, testis and brain) were removed quickly, and total RNA was isolated. cDNA was synthesised by the Superscript First-Strand Synthesis System for RT-PCR

(Invitrogen), after RNA quantification and quality proofing. Mouse GLUT8 exon–intron organisation is known and we designed specifics primers for GLUT8 cDNA amplification. The sense and antisense primers were (5′-TGACATGTCTCC-CGAGGACC-3′), and (5′-TTTCCCAGACAGTAGCAGG-3′), both located on exon I and X, respectively. PCR products were cloned using the TOPO cloning system (Invitrogen), and cDNA sequences determined by sequencing. Southern blot analysis was performed to examine the alternative splicing of GLUT8. RT-PCR products generated were treated with 40 U S1 nuclease (Roche), and after agarose (2 %) gel electrophoresis transferred to nitrocellulose, and then hybridised with a GLUT8 cDNA probe.

To study GLUT8 expression on small intestine and to compare with other tissues, RT-PCR screening was performed from total RNA tissues using two sets of primers (amplified from the N-terminus to the C-terminus). We have found that GLUT8 is expressed in all tissues screened (1438 pb), small intestine included. Moreover, in small intestine, in addition to the full length, we have found several alternative splicing transcripts of mouse GLUT8 as a product of specific exon deletion. We do not know yet the specific role of these transcripts in the small intestine, but they could be a specific mechanism in order to regulate GLUT8 expression in this tissue and contribute to the intestinal sugar absorption under specific conditions.

Carayannopoulos MO *et al.* (2002). *Proc Natl Acad Sci USA* **97**, 7313–7318.

Doege H *et al.* (2000). *J Biol Chem* **275**, 16275–16280.

Ibberson M *et al.* (2000). *J Biol Chem* **275**, 4607–4612.

This work was supported in part by grants from Ministerio de Ciencia y Tecnología BFI2002-03590, and from University of Cardenal Herrera-CEU PRUCH02/18.

All procedures accord with current National guidelines.

P35

Effect of kefir milk on intestinal dissacharidase activities in brush-border membrane vesicles

E. Urdaneta, P. Aranguren, S. García, F. Ibañez and F. Marzo

Laboratory of Animal Physiology and Nutrition, Public University of Navarra, 31006 Pamplona, Spain

Probiotics are foods that contain live bacteria, which are beneficial to health. Kefir is a stirred beverage made from milk fermented with a complex mixture of bacteria, including various species of lactobacilli, lactococci, leuconostocs and aceterobacteria and yeasts (both lactose-fermenting and non-lactose-fermenting) (Thoreux & Schmucker, 2001). A number of studies suggest stimulation of immune function and suppression of cancer by consumption of probiotics, as well as improved intestinal microbial balance (Collins & Gibson, 1999).

The aim of the present study is to report data about effects of kefir on enzymes and proteins of the gut. Kefir was incubated with pepsin (20 mg (g protein)$^{-1}$) after acidification to pH 2.5 with HCl, and this mixture was mixed for 1 or 2 h at 37 °C. The proteolysis was stopped by neutralization of pH by NaOH addition. Nitrogen content was measured by the Kjeldahl method. Jejunal brush-border membrane vesicles (BBMV) were isolated from adult pigs (humanely killed) by the method of Shirazy-Beechey *et al.* (1990). After protein determination BBMV were incubated with digested kefir for 30 min at 37 °C. Intestinal sucrase and maltase activities were determined in control and with kefir conditions by the methold of Dahlqvist (1964).

The protein quantity of kefir and kefir digested for 1 or 2 h was 2.89, 1.47 and 1.76 %, respectively. Sucrase activity was diminished ($P < 0.05$, Student's paired t test) after incubation of digested kefir for 2 h and maltase activity was also reduced ($P < 0.05$) with the probiotic.

These data indicate that kefir intake appears to modify the intestinal disaccharidase activities due to the bioactive components. Further studies are needed to confirm this conclusion.

Collins MD & Gibson GR (1999). *Am J Clin Nutr* **69**, 1052–1057S.

Dahlqvist A (1964). *Anal Biochem* **7**, 18–25.

Shirazy-Beechey SP *et al.*(1990). *Gastroenterology* **98**, 676–685.

Thoreux K & Schmucker DL (2001). *J Nutr* **131**, 807–812.

This work was supported by the Government of Navarra.

All procedures accord with current National guidelines.

P36

Nutritional response of laboratory animals to faba beans (*Vicia faba* L. var. Aguadulce) diets

F. Marzo, E. Urdaneta, C. Chocarro, F. Ibañez and S. Santidrián

Laboratory of Animal Physiology & Nutrition, Public University of Navarra, 31006 Pamplona, Spain

A feeding experiment was conducted with growing male Wistar rats to determine the effects of extruded faba bean (*Vicia faba*) on *in vivo* and *in vitro* intestinal absorption of D-galactose. The extrusion process abolishes haemagglutinating activity, trypsin, chymotrypsin and α-amylase inhibitory activity (Gujska & Khan, 1990). Condensed tannins and phytic acid content were also reduced significantly after processing (Liener, 1994).

Rats were fed raw faba beans (RFB) or an extrusion diet (EFB). A significant ($P < 0.05$, Student's paired t test) impairment in growth rate and a significant ($P < 0.05$) inhibition *in vivo* and *in vitro* of intestinal absorption of galactose were found in raw faba beans (RF)-fed rats compared with casein (C)-fed rats. Moreover, extruded faba bean (EFB)-fed rats showed a significant ($P < 0.05$) improvement in growth rate and a significant increase ($P < 0.001$) in the rate of *in vivo* and *in vitro* intestinal absorption of D-galactose compared with RF and RFB groups, respectively. Animals fed with extruded legume-based diets showed a marked decrease in growth and a reduced *in vivo* and *in vitro* intestinal absorption of D-galactose compared with C rats.

The raw faba bean diet produced a 59 % inhibition ($P < 0.001$, Student's paired t test) of 2 mM D-galactose uptake by intestinal rings. But the same extruded blend only produced an 18 % inhibition ($P < 0.001$) of the sugar intestinal uptake. Both inhibitions were different ($P < 0.01$). The inhibition was not completely abolished by thermal processing, suggesting that the remaining antinutritional factors after extrusion could be responsible for the reported effects. Gross denaturing of the glycocalix and of the brush border of the epithelial intestinal cells or the formation of complexes between some of faba bean components and nutrients are some of the mechanisms proposed by different investigators to explain these inhibitory effects.

Gujska E & Khan K (1990). *J Food Sci* **55**, 466–469.

Liener IE (1994). *Crit Rev Food Sci Nutr* **34**, 31–67.

This work was supported partially by the Spanish DGICYT97-0675 project.

All procedures accord with current National guidelines.

P37

Characterization of the rat Na^+–nucleoside cotransporter (rCNT2) using electrophysiological methods

I.M. Larráyoz and M.P. Lostao

Departamento de Fisiología y Nutrición, Universidad de Navarra, Pamplona, Spain

The purine-preferring Na^+–nucleoside cotransporter (rCNT2) was cloned from a rat blood–brain barrier cDNA library (Yi Li *et al.* 2001). In the present work, we have expressed rCNT2 in *Xenopus laevis* oocytes and used the two-electrode voltage-clamp method (Loo *et al.* 1993; Lostao *et al.* 1994; Díez-Sampedro *et al.* 2001) to study the substrate specificity, kinetics properties of Na^+ and substrate as a function of voltage and stoichiometry.

The apparent affinity constant ($K_{0.5}$), at −50 mV membrane potential (V_m), for adenosine, guanosine and uridine was 13.8 ± 2.5 (S.E.M.), 23.5 ± 2 and 14.8 ± 6.1 μM, respectively, and the maximal current (I_{max}) was similar for the three nucleosides. Inosine, the cellular precursor of purine nucleosides, showed a $K_{0.5}$ of 31.2 ± 1.5 μM and an I_{max} half of that for adenosine. As expected, the pyrimidine nucleosides thymidine and cytidine did not induce any Na^+ inward current or inhibited the uptake of 50 μM uridine, indicating that they do not interact with the transporter. Similarly, the pyrimidine-derived anticancer drugs gemcitabine and 5′-deoxy-5-fluorouridine do not induce any inward current. Two purine-derived drugs were also investigated. Fludarabine, currently used in the treatment of lymphoproliferative malignancies, exhibited an I_{max} 2-fold higher than that for adenosine and an affinity one order of magnitude lower than the adenosine affinity ($K_{0.5}$ = 378.1 ± 82.6 μM). Formycin B, used in the treatment of parasitic diseases, showed a $K_{0.5}$ of 66 ± 6.5 μM and an I_{max} also 2-fold higher than the adenosine I_{max}. For all substrates tested, I_{max} increased as the membrane potential was hyperpolarized from −10 to −150 mV, whereas $K_{0.5}$ was not affected by the membrane potential between −30 and −150 mV. The apparent affinity constant for Na^+ was also independent of membrane potential (0.7 ± 0.2 mM at −150 mV and 1.3 ± 0.5 mM at −30 mV).

To determine the charge-to-nucleoside stoichiometry, radio-labelled substrate influx was measured under voltage-clamp conditions (V_m = −50 mV) resulting in two inward positive charges (most likely due to Na^+) per molecule of transported nucleoside.

Finally, experiments performed in Na^+ buffer in the absence of substrate, after rapid steps in membrane potential, revealed the presence of pre-steady-state currents which indicate charge transfer associated to the movement of the transporter in the membrane. The analysis of these currents will be useful to understand the mechanism of this transporter.

Díez-Sampedro A *et al.* (2001). *Am J Physiol Renal Physiol* **49**, F278–282.

Loo DDF *et al.* (1993). *Proc Natl Acad Sci USA* **90**, 5767–5771.

Lostao MP *et al.* (1994). *J Memb Biol* **142**, 161–170.

Yi Li L *et al.* (2001). *J Cereb Blood Flow Metabol* **21**, 929–936.

This work was supported by PIUNA (University of Navarra) and 'Departamento de Educacíon y Cultura' (Navarra Government).

P38

In vivo sugar diffusion in the ileal epithelium of spontaneously hypertensive rats

A. Mate, L. Gómez-Amores, C.M. Vázquez and J. Bolufer

Department of Physiology and Zoology. University of Seville, c/Tramontana s/n, E-41012 Seville, Spain

D-Glucose absorption, distinguishing between active and diffusive components, has been studied in the ileum of spontaneously hypertensive rats (SHR) and their normotensive control, Wistar-Kyoto (WKY) rats, using a perfusion system *in vivo* (Vinardell & Bolufer, 1983). In addition, net water transport has also been determined. Twelve-week-old rats were fasted for 18 h and anaesthetised with urethane (1.25 g (kg body weight)$^{-1}$) before performing a laparotomy; they were humanely killed at the end of the experiment. A significant decrease in total D-glucose absorption was found in SHR when compared to WKY rats, this reduction being due to a lower SGLT1-mediated component. This effect was not compensated by the total diffusive component, since the phlorizin-insensitive D-glucose absorption did not significantly change between the two rat strains. However, the diffusive component of D-glucose transport was relatively more important in hypertensive than in normotensive rats. The use of 2,4,6-triaminopyrimidine (TAP), which blocks the transport across the paracellular route, showed that the paracellular diffusion of D-glucose was higher in SHR than in WKY rats. On the other hand, intestinal net water transport was not modified between the two groups of animals, though the presence of phlorizin in the perfusate decreased the ileal water absorption to a greater extent in normotensive rats. Moreover, the addition of TAP produced a higher inhibition on the net water transport in WKY than in SHR, thus indicating that the transcellular transport of water is higher in hypertensive rats. In conclusion, the observed reduction in D-glucose absorption *in vivo* in the ileum of SHR was due to a decrease in the active, SGLT1-mediated component. The total D-glucose diffusive component did not compensate for this effect, although the paracellular diffusion of D-glucose was quantitatively higher in hypertensive than in normotensive rats.

Vinardell MP & Bolufer J (1983). *J Physiol Biochem* **39**, 193–196.

This work was supported by grants from Ministerio de Sanidad, Fondo de Investigaciones Sanitarias (FIS 97/1143 and 99/1142). L. Gómez-Amores was supported by a grant from Sigma-Tau Laboratory.

All procedures accord with current National and local guidelines.

P39

Expression and localization of aquaporin water channels in human exocrine pancreas

B. Burghardt*, M.-L. Elkjær†, T.-H. Kwon‡, G.Z. Rácz*, G. Varga*§, M.C. Steward¶ and S Nielsen†

**Institute of Experimental Medicine, Hungarian Academy of Sciences, Budapest, Hungary, †The Water and Salt Research Center, University of Aarhus, Denmark, ‡Department of Physiology, Dongguk University School of Medicine, Korea, §Department of Oral Biology, Semmelweis University, Budapest, Hungary and ¶School of Biological Sciences, University of Manchester, UK*

The exocrine pancreas secretes large volumes of isotonic, bicarbonate-rich fluid, much of which originates from the ductal system. Since the role of aquaporin (AQP) water channels in this

process is unknown, we have investigated the expression and localization of known AQP isoforms in normal human pancreas and in pancreatic cell lines of ductal origin (Capan-1, Capan-2 and HPAF).

RT-PCR was performed with isoform-specific primers on RNA extracted from tissue samples obtained from patients undergoing surgery who had previously given consent according to local procedures. Immunohistochemistry was performed on paraffin sections using affinity-purified antibodies and peroxidase-linked or fluorescent secondary antibodies.

Messenger RNAs for AQP1, -3, -4, -5 and -8 were detected in normal pancreas by RT-PCR. The ductal cell lines expressed AQP3, -4 and -5 but lacked AQP1 and AQP8. Immunohistochemistry of normal pancreas revealed that AQP1 is strongly expressed in the centro-acinar cells and in both the apical and basolateral domains of the intercalated and intralobular duct epithelia. AQP1 expression declined with distance along the small interlobular ducts and was not detectable in the larger interlobular ducts. This is in contrast to the rat pancreas where AQP1 is found mainly in the interlobular ducts (Ko *et al.* 2002). AQP3 and AQP4 were not detectable in human pancreas by immunohistochemistry despite the positive RT-PCR results. AQP5 was observed at the apical membrane of the intercalated duct cells and also in duct-associated mucoid glands. AQP8 was confined to the apical pole of the acinar cells, as previously observed in the rat pancreas (Hurley *et al.* 2001). Using immunofluorescence, both AQP1 and AQP5 were co-localized with CFTR at the apical membrane of the intercalated duct cells.

We conclude that AQP1 and AQP5 are strongly expressed in the intercalated ducts of the human pancreas, and that their distribution correlates closely with that of CFTR, a marker of ductal electrolyte secretion. This suggests that fluid secretion occurs predominantly in the terminal branches of the ductal tree and that both AQP1 and AQP5 may be involved.

Hurley PT *et al.* (2001). *Am J Physiol* **280**, G701–709.
Ko SBH *et al.* (2002). *Am J Physiol* **282**, G324–331.

This study was supported by Danish National Research Foundation, the Hungarian Ministry of Social Welfare and the Wellcome Trust.

All procedures accord with current local guidelines and the Declaration of Helsinki.

P40
Acid secretion by intact distal airways

S.K. Inglis and S.H. Ross

Tayside Institute of Child Health, University of Dundee, Dundee DD1 9SY, UK

Secretion of HCO_3^- by airway submucosal glands is essential for normal liquid and mucus secretion (Inglis *et al.* 1998). Since the liquid bathing the airway surface is fairly acidic, we have proposed that the surface epithelium may acidify HCO_3^--rich glandular fluid. The aim of this study was to investigate the mechanisms by which intact distal airways acidify luminal fluid.

Distal bronchi were isolated from humanely killed pigs, cannulated in a bath containing HCO_3^- buffered solution and perfused (3 ml min^{-1}) with similar solution, in which NaCl replaced $NaHCO_3^-$. This solution was lightly buffered (buffering capacity 0.6 mM (pH unit)$^{-1}$) with KH_2PO_4 and NaOH to pH ~7, gassed with 100% O_2 to eliminate dissolved CO_2 and stirred vigorously. The pH of this circulating luminal solution (10 ml) was monitored continuously. Upon perfusion through the airway lumen pH initially fell by 0.053 ± 0.005 pH units ($[H^+]$ increase 1.56 ± 0.19 μmol h^{-1}; means ± S.E.M., $n = 22$) before stabilising (see Fig. 1). This acidification was unaffected by luminal dimethylamiloride (100 μM), a Na^+/H^+ exchange inhibitor, but was significantly inhibited (75.9 ± 13.3%, $n = 5$, Student's paired t test $P < 0.05$) by bafilomycin A_1 (100 nM), a blocker of vH^+-ATPase. Alkalinisation of the circulating solution by addition of NaOH induced further acidification, whose magnitude was dependent on the magnitude of the induced alkalinisation. Further analysis of these data using empirically determined buffering capacity of the circulating solution showed that the rate of secretion of acid equivalents was unaffected by the magnitude of alkalinisation. Fischer *et al.* (2002) recently showed that apical ATP significantly increased luminal acidification through proton conductances in cultured proximal airways. However, inclusion of ATP (100 μM) in the unbuffered luminal solution perfusing distal bronchi significantly reduced luminal acidification. After 20 min perfusion, the pH of control luminal buffer had fallen by 0.060 ± 0.008 units, whilst the pH of buffer containing ATP had acidified by only 0.023 ± 0.016 units ($n = 10$, $P < 0.05$).

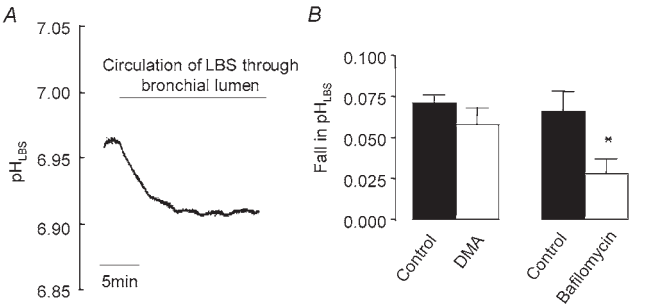

Figure 1. *A,* acidification of lightly buffered solution (LBS) upon circulation through bronchial lumen. *B,* effect of dimethylamiloride (DMA) (100 μM) and bafilomycin A1 (100 nM) on fall in pH_{LBS}.

These data suggest that intact distal bronchi acidify their lumen through activity of vH^+-ATPase. This acidification can be induced by alkalinisation of the lumen, and is not stimulated by luminal ATP.

Fischer H *et al.* (2002). *Am J Physiol* **282**, C736–C743.
Inglis SK *et al.* (1998). *Am J Physiol* **274**, L762–L766.

This work was supported by the Wellcome and Tenovus Trusts.

All procedures accord with current UK legislation.

P41
$P2Y_1$, $P2Y_2$ and $P2Y_4$ receptor localisation in human hyperhidrotic eccrine sweat glands

S.L. Lindsay*, R. Holdsworth† and D.L. Bovell*

**School of Life Sciences, Glasgow Caledonian University, Glasgow G4 0B and †Department of Vascular surgery, Stirling Royal Infirmary, Glasgow, UK*

The purinoceptor agonist ATP has been shown to induce sweating in isolated glands (Sato *et al.* 1991) and to increase intracellular calcium in primary cultures of human glands (Bovell *et al.* 2000). These findings have indicated the presence of a P2Y receptor and recently we have localised three receptor

subtypes in normal human glands (Lindsay *et al.* 2002). Although the function of purinoceptors is still elusive, their presence in normal glands suggests they have a role in sweat secretion. Hyperhidrosis, a condition characterised by the production of an inappropriately large volume of sweat, may have purinoceptor involvement. The presence of such receptors in hyperhidrotic glands has, to our knowledge, not been investigated and therefore immunohistochemistry was employed to investigate the localisation and possible differing distribution of the $P2Y_1$, $P2Y_2$ and $P2Y_4$ subtypes, in human hyperhidrotic eccrine sweat glands.

Skin biopsies were obtained by informed consent and with local medical ethical committee approval, from both male and female patients, with the condition hyperhidrosis. Samples were fixed (10 % buffered formalin) and processed using standard techniques. Immunohistochemical staining was performed using rabbit antibodies raised against $P2Y_1$, $P2Y_2$ and $P2Y_4$ (Alomone Labs, Israel), employing the avidin–biotin complex (ABC) procedure (Vector Labs, UK). Sections were counterstained with haematoxylin, dehydrated, cleared, mounted and viewed using light microscopy.

In all samples analysed, the eccrine reabsorptive duct of hyperhidrotic glands was shown to contain dark $P2Y_1$-, $P2Y_2$-and $P2Y_4$-like immunoreactivity localised to the apical membrane ($n = 6$, $n = 8$ and $n = 5$, respectively), which was similar to that found in normal glands. However, hyperhidrotic glands exhibited staining throughout the basolateral membranes with all three antibodies, which was not seen in normal glands. The secretory coil of hyperhidrotic sweat glands was shown to have staining localised to what looks to be the light cells of the coil with $P2Y_1$, $P2Y_2$ and $P2Y_4$ ($n = 4$). This pattern of staining was only seen in normal glands with $P2Y_4$ antibody and not with the other two subtypes. Immunoreactivity was localised to the outer myoepithelial cells with $P2Y_1$ and $P2Y_2$ ($n = 4$ and $n = 7$) in both normal and hyperhidrotic glands. Preabsorption of the antibodies with the appropriate control peptide abolished all specific staining.

The presence of apical purinoceptors in the duct of hyperhidrotic glands is similar to that of normal glands and is suggestive of apical regulation of absorption. Hyperhidrotic sweat glands showed an increased distribution of the P2Y receptor subtypes compared to normal glands. These receptors may be present to help reabsorb as much fluid as possible and prevent drastic salt loss. The clear cells of the secretory coil are the ones predominantly involved in sweat secretion and the localisation of all three subtypes in these cells of hyperhidrotic glands suggests that these receptors are implicated in sweat secretion and could play a role in the condition hyperhidrosis. The myoepithelial cells of the sweat gland are not regarded as cells involved in either secretion or reabsorption of sweat and the presence of purinoceptors requires further investigation.

Bovell DL *et al.* (2000). *Pflugers Arch* **403**, 45–48.

Lindsay S *et al.* (2002). *J Physiol* **543P**, 92*P*.

Sato K *et al.* (1991). In *Pathophysiology of Dermatologic Diseases,* 2nd edn, pp. 211–234.

S.L.L is supported by a GCU studentship.

All procedures accord with current local guidelines and the Declaration of Helsinki.

P42

The K^+–Cl^- cotransporter (KCC1) is expressed in rat pancreatic α-cells

Eleni Roussa*, Philippe Le Rouzic, Sarah L. Davies, Seth Alper† and Peter D. Brown

*School of Biological Sciences, University of Manchester, Manchester M13 9PT, UK, *Department of Neuroanatomy, Georg-August-University, Gottingen, Germany and †Harvard Medical School, Boston, MA 02215, USA*

We have recently reported functional evidence for the expression of K^+–Cl^- cotransporters in rat pancreatic α-cells (Davies *et al.* 2002). In the present study we have investigated the expression of the KCC1 isoform of K^+–Cl^- cotransporter in pancreatic islets.

Sprague-Dawley rats were killed humanely by stunning and cervical dislocation. RT-PCR was performed on RNA isolated from the pancreas, using primers designed to amplify the rat KCC1 isofom. A product of the expected size (320 kb) was obtained, which when sequenced showed 100 % identity with the published sequence for rat KCC1. The location of KCC1 expression in the exocrine pancreas was examined by immunocytochemical methods, using an antibody raised against the N-terminus of mouse KCC1 (Roussa *et al.* 2002). Primary antibody binding to 5 μm cryosections of rat pancreas was detected using fluorescently labelled secondary antibodies.

KCC1 expression was confined to cells on the periphery of the islets of Langerhans. In co-localisation studies, KCC1 expression was observed in glucagon-staining cells, but not in cells staining for insulin or somatostatin. Immunocytochemistry performed in isolated islet cells identified KCC1 only in the smaller cells of the preparation (volume 0.43 ± 0.06 pl; mean ± S.E.M., $n = 26$), which are known to be α-cells (Majid *et al.* 2001).

In conclusion, we have shown that KCC1 mRNA and protein are present in rat pancreas. Furthermore, KCC1 appears only to be expressed in the α-cells of the endocrine pancreas.

Davies SL *et al.* (2002). *J Physiol* **544.P**, 91*P*.

Majid A *et al.* (2001). *Pflugers Arch* **442**, 570–576.

Roussa E *et al.* (2002). *Histochem Cell Biol* **117**, 335–344.

S.L.D. is supported by the MRC and P.L. is supported by the BBSRC.

All procedures accord with current UK legislation.

P43

Acetylcholine stimulates secretion of chloride and bicarbonate through cystic fibrosis transmembrane conductance regulator in an airway epithelial cell line

L. Finlay, S.K. Inglis, S.M. Wilson and R.E. Olver

Tayside Institute of Child Health, Ninewells Hospital and Medical School, Dundee

Cystic fibrosis (CF), a lethal genetic disease, leads to disruption of ion and fluid transport across the airway epithelium, with early, severe pathological changes occurring in the submucosal glands. Inhibition of both chloride and bicarbonate secretion prior to stimulation with the glandular secretagogue acetylcholine leads to mucus occlusion of the glands, resembling the changes seen in CF (Inglis *et al.* 1997). However, the exact mechanisms underlying ion transport in these glands are not known. Calu-3 human airway epithelial cells exhibit many features of the serous cells of the submucosal glands. When grown to confluence on

Snapwells and mounted in Ussing chambers, they demonstrate an increase in short circuit current (I_{sc}) in response to acetylcholine (ACh) (M.C. Constable, unpublished data). This study investigates the ion transport processes involved in this response.

Calu-3 cells were grown to confluence on Snapwell filters (10 days approximately) before being mounted in Ussing chambers in a HCO_3^-/CO_2 buffer. The effect on short circuit current of 100 μM ACh (basolateral) was noted after pre-treatment with either an anion channel blocker (glibenclamide, diphenylamine-2-carbonsaeure (DPC), or 4,4′-diisothiocyanato-stilbene-2,2′-disulfonic acid (DIDS)) or apical dimethylsulfoxide (DMSO). Glibenclamide and DPC are blockers of cystic fibrosis transmembrane conductance regulator (CFTR), while DIDS blocks other chloride channels but not CFTR. Glibenclamide pre-treatment resulted in a 37.2 ±11.7 % (mean ± S.E.M.) inhibition of ACh-stimulated I_{sc} compared to DMSO ($n = 8$, $P = 0.03$, Student's paired t test, used in all statistical analysis). DPC caused an inhibition of 43.9 ± 15.6 % of the ACh response ($n = 8$, $P = 0.02$). However, DIDS caused no significant reduction in I_{sc} ($n = 8$, $P = 0.68$). These blocker sensitivities suggest that the response of Calu-3 cells to ACh is mediated through CFTR.

There was no significant difference between the responses to ACh in Hepes-Krebs solution and HCO_3^-/CO_2 buffers ($n = 6$, $P = 0.38$). When a Cl^--free HCO_3^- solution was used instead of a Cl^--containing HCO_3^-solution, the response to ACh was reduced by 53.6 ± 11.5 % ($n = 9$, $P = 0.009$), suggesting that the response to ACh in Cl^--containing buffer is at least partly mediated by Cl^- secretion across the apical membrane. When a Cl^--free Hepes solution was used, the response to acetylcholine was reduced by 82.8 ± 4.1 % relative to Cl^--containing Hepes ($n = 9$, $P = 0.00003$). This supports the hypothesis that HCO_3^- is secreted in response to acetylcholine in HCO_3^-/CO_2 buffered solutions, and is responsible for approximately two-thirds of the residual current in Cl^--free HCO_3^- buffer.

Inglis SK *et al.* (1997). *Am J Physiol* **272**, L372–377.

This work was supported by the Medical Research Council.

P44

Acetylcholine-evoked anion secretion across tracheal epithelium

M.C. Constable, E.M. Husband and S.K. Inglis

Tayside Institute of Child Health, University of Dundee, Dundee DD1 9SY, UK

Previous studies have shown that acetylcholine (ACh) evokes an increase in short circuit current (I_{sc}) and transepithelial potential difference (PD) across isolated distal bronchi that is unaffected by inhibition of either Cl^- or HCO_3^- secretion but is blocked if both pathways are inhibited (Inglis *et al.* 1996). These data suggest that ACh stimulates both Cl^- and HCO_3^- secretion and that the independent inhibition of secretion of one anion augments secretion of the other. The aim of the present study was to investigate whether ACh-induced anion secretion in tracheal epithelium is similar to that described in bronchi.

Tracheas were removed from humanely killed pigs and the epithelial layer dissected from underlying cartilage. Epithelia were mounted in modified Ussing chambers and bathed in HCO_3^- buffered solution, gassed with 95 % O_2–5 % CO_2 at 37°C. Serosal ACh (10 μM) stimulated a peak increase in I_{SC} (17.7 ± 2.9 μA cm^{-2}, mean ± S.E.M., $n = 5$) that slowly decayed with time. The response of paired epithelia bathed in Hepes-buffered solution containing acetazolamide (10 mM), to inhibit carbonic anhydrase, was not significantly different (20.3 ± 1.6 μA cm^{-2}, Student's paired t test used throughout, $P = 0.55$), showing that inhibition of HCO_3^- secretion alone has no effect on the response to ACh. Bumetanide (10 μM, serosal), however, significantly inhibited the response to ACh (81.7 ± 7.4 %, $n = 5$, $P < 0.05$), demonstrating that inhibition of Cl^- secretion alone is sufficient to block the response to ACh in tracheal epithelium. Apical addition of the anion channel blockers DPC (1 mM) and NPPB (300 μM) also significantly reduced the response to ACh (by 60.1 ± 14.8 % ($n = 9$) and 80.1 ± 10.5 % ($n = 7$) respectively, $P < 0.05$), whilst DIDS had no effect ($P > 0.05$, $n = 7$). Basolateral addition of DIDS, however, significantly reduced the response to ACh (33.1 ± 12.3 %, $n = 10$, $P < 0.05$), whilst DNDS had no significant effect ($n = 7$, $P > 0.05$). These results suggest that the majority of the electrogenic response to ACh in tracheal epithelium results from stimulation of Cl^- secretion. Involvement of HCO_3^- secretion is suggested, however, by the inhibitory effect of DIDS, which may block HCO_3^- uptake across the basolateral membrane via anion exchange. To investigate this further, we measured the effect of ACh on the pH of HCO_3^--free, unbuffered solution placed in the luminal side of the Ussing chamber. The mean rate of secretion of base equivalents into the luminal chamber was significantly increased by ACh addition from −0.44 ± 0.09 μmol h^{-1} for the 10 min prior to ACh addition to 0.59 ± 0.13 μmol h^{-1} for 10 min after ACh addition ($n = 13$, $P < 0.05$). This is consistent with ACh-evoked stimulation of HCO_3^- secretion into the luminal chamber.

In summary, ACh stimulates I_{SC} across porcine tracheal epithelium. In contrast to its effect on bronchial epithelium, the majority of this I_{SC} results from stimulation of Cl^- secretion. HCO_3^- secretion is also evoked by ACh, and this may partly be via an electroneutral mechanism.

Inglis SK *et al.* (1996). *Am J Physiol* **270**, L289–297.

This work was supported by the Wellcome and Tenovus Trusts

All procedures accord with current UK legislation.

P45

The morphologically differentiated human colonic cell line LIM1863 shows CFTR-dependent Cl^- secretion and ENaC-dependent Na^+ absorption

Aoife Currid*† Bernardo Ortega† and Miguel A. Valverde†

**GKT School of Medicine and Dentistry, King's College London, UK and †Cell Signalling Unit, Universitat Pompeu Fabra, Barcelona, Spain*

Cell line models of colonic electrolyte transport have been used extensively, despite lacking some characteristics of the native tissue. While native colonic crypts absorb or secrete NaCl, immortalized cell lines only retain the secretory phenotype. In this study we characterized functionally and molecularly fluid and electrolyte transport in the morphologically differentiated human colonic cell line LIM1863 (Whitehead *et al.* 1987).

Net fluid transport was evaluated by the morphometric measurement of lumens (expressed in pixels) formed in LIM organoids in response to secretagogues. To normalize the differences in organoid size, the lumen area was divided by the initial organoid radius. Functional profiling of the channels and transporters involved in fluid and electrolyte transport was determined pharmacologically, while the molecular basis was determined by RT-PCR and/or immunofluorescence confocal microscopy.

Similar to native tissue, LIM1863 cells secrete fluid and electrolytes across the apical membrane into a central lumen when exposed to cAMP-mediated secretagogues such as forskolin (10 μM, lumen size 82 ± 3 pixels (mean ± S.E.M.); $n = 95$). Lumen formation was markedly reduced by 100 μM azosemide (29 ± 2 pixels; $n = 33$), consistent with Cl^- uptake across the basolateral membrane through a Na^+–K^+–$2Cl^-$ cotransporter. Cl^- exit across the apical membrane into the lumen appears to be via the cystic fibrosis transmembrane conductance regulator (CFTR) Cl^- channel, as the lumen formation was reduced by 100 μM glibenclamide, an inhibitor of CFTR (42 ± 3 pixels; $n = 21$) but unaffected by 100 μM DIDS (83 ± 6 pixels; $n = 11$), an inhibitor of Ca^{2+}-activated Cl^- channels.

Electrogenic NaCl absorption occurs throughout the human colon, and involves the aldosterone-regulated epithelial sodium channel (ENaC) (Sandle, 1989). Colonic cell lines are thought to lack ENaC due to their insufficient level of differentiation (Greger, 2000). Interestingly, we have shown that LIM1863 cells express ENaC (RT-PCR and immunocytochemistry studies) and reduce their lumen size attributable to NaCl absorption, a response that is increased significantly by aldosterone (1 μM; $P < 0.001$ *vs.* control, unpaired *t* test). To our knowledge, this is the first example of the functional expression of ENaC in a colonic epithelial cell line, introducing LIM1863 cells as a new model for further delineation of colonic secretion and absorption.

Greger R (2000). *Annu Rev Physiol* **62**, 467–491.

Sandle GI (1989). *Pflugers Arch* **414**, 706–712.

Whitehead RH *et al.* (1987). *Cancer Res* **47**, 2683–2689.

This work was funded by Ministerio de Ciencia y Tecnología (Spain) and The King's Medical Research Trust, UK.

P46

Effect of protein kinase A and protein kinase C inhibition on carbachol-induced short circuit current (I_{SC}) in rat distal colon

M. Bellingham, D. Bovell and A.D. Corbett

Department of Biological and Biomedical Sciences, School of Life Sciences, Glasgow Caledonian University, Cowcaddens Road, Glasgow G4 0BA, UK

The muscarinic receptor agonist carbachol evokes Cl^- secretion in rat colonic epithelial cells by increasing intracellular Ca^{2+} (Greger *et al.* 1997). Previous studies from our laboratory have shown that carbachol-induced anion secretion in rat distal colon is predominantly through cystic fibrosis conductance regulator (CFTR) channels (Bellingham *et al.* 2002*a*), regulated by protein kinase phosphorylation and intracellular cAMP (Jia *et al.* 1997; Dahan *et al.* 2001). Here we have examined the involvement of protein kinases A and C (PKA and PKC) in carbachol-induced I_{SC} in rat distal colon.

The terminal colon (5 cm) was removed from male Wistar rats humanely killed by cervical dislocation. The mucosal portion was mounted in an Ussing chamber (area 0.5 cm^2) containing Krebs solution (mM: NaCl 119, KCl 4.7, $NaHCO_3$ 24.8, $MgSO_4$ 1.2, KH_2PO_4 1.2, $CaCl_2$ 2.5 and glucose 11.1) at 37°C gassed with 95 % O_2–5 % CO_2. Short circuit current (I_{SC}) was recorded and measurements taken from baseline to peak. All values are means ± S.E.M. and Student's paired *t* test was used to test significance ($P < 0.05$).

Basal I_{SC} was 5.2 ± 3.2 μA cm^{-2} ($n = 20$). Carbachol (100 μM basolateral) stimulated a triphasic response consisting of an increase in I_{SC} (phase 1, 8.7 ± 3.2 μA cm^{-2}) followed by a decrease towards baseline (phase 2, 4.9 ± 4.8 μA cm^{-2}) then a large increase (phase 3, 92.0 ± 14.3 μA cm^{-2}, $n = 5$) that decayed to a stable plateau. We have previously shown that phases 1 and 3 of the carbachol-induced I_{SC} are caused by Cl^- and HCO_3^- secretion (Bellingham *et al.* 2002*b*). In the presence of the PKA inhibitor H-89 (Sigma, 100 μM apical) phase 3 of the carbachol-induced I_{SC} was significantly reduced but phases 1 and 2 were unaltered (phase 1, 6.8 ± 2.0 μA cm^{-2}; phase 2, 1.1 ± 1.7 μA cm^{-2}; phase 3, 42.3 ± 6.5 μA cm^{-2}, $P < 0.05$, $n = 5$). In the presence of the adenylate cyclase inhibitor MDL 12330A (Sigma, 100 μM basolateral and apical), phase 3 of the carbachol response was also significantly reduced compared to control (phase 1, 7.0 ± 2.1 μA cm^{-2}; phase 2, −8.4 ± 0.8 μA cm^{-2}; phase 3, 31.2 ± 2.4 μA cm^{-2}, $P < 0.05$, $n = 5$). However, in the presence of the PKC inhibitor chelerythrine chloride (Sigma, 100 μM apical) the triphasic carbachol response was unaffected ($n = 5$).

The present results would suggest that carbachol-induced anion secretion in the rat distal colon occurs partly through activation of cAMP-dependent PKA, which is a potent activator of CFTR (Dahan *et al.* 2001) since both adenylate cyclase and PKA inhibition reduced the carbachol-induced I_{SC}. PKC inhibition had no significant effect on the carbachol-induced I_{SC} suggesting that PKC plays a negligible role compared to PKA in carbachol-induced ion secretion in rat distal colon.

Bellingham M *et al.* (2002*a*). *J Physiol* **544.P**, 102*P*.

Bellingham M *et al.* (2002*b*). *J Physiol* **543.P**, 52*P*.

Dahan D *et al.* (2001). *Pflugers Arch* **443**, S92–S96.

Greger R *et al.* (1997). *Comp Biochem Physiol* **118**, 271–275.

Jia Y *et al.* (1997). *J Biol Chem* **272**, 4978–4984.

MB is supported by a GCU studentship

All procedures accord with current UK legislation.

P47

Regulation of an outwardly rectifying Cl^- conductance in mouse inner medullary collecting duct (mIMCD-3) cells

J.E. Linley, M.A. Gray and N.L. Simmons

School of Cell and Molecular Biosciences, Medical School, Framlington Place, University of Newcastle upon Tyne, Newcastle upon Tyne NE2 4HH, UK

Our previous studies using renal inner medullary collecting duct cells (IMCD-3 cell-line) have identified the presence of a large spontaneously active apical Cl^- conductance (Stewart *et al.* 2001) that is increased upon elevation of intracellular calcium ($[Ca^{2+}]_i$) by kinins, and external ATP (Stewart *et al.* 2001). In order to more directly confirm the regulation and sensitivity of the IMCD anion conductance to $[Ca^{2+}]_i$, fast whole cell patch clamp experiments were conducted with a pipette solution (pH 7.2), containing (mM) TEA Cl (110), $MgCl_2$ (2), ATP (1) and EGTA (5) in which $CaCl_2$ was added to give buffered free $[Ca^{2+}]_i$ values of 10, 300 and 1000 nM. Cells were initially bathed in a Na^+-rich Krebs solution (2.8 mM Ca^{2+}) and voltage clamped using a 10 s cycle with the holding potential (V_{hold}) at 0 mV with 500 ms excursions to ± 60 mV.

At 10 nM $[Ca^{2+}]_i$, initial (1.5 min after establishing whole-cell) recordings demonstrated an outwardly rectifying current (current densities ± 60 mV, 59 ± 13 pA pF^{-1} −32 ± 8 pA pF^{-1} (means ± S.E.M.), $n = 11$ respectively) with an E_{rev} of −8.1 ± 0.6 mV, close to the estimated Cl^- equilibrium potential of −8.7 mV). At 5 min mean current densities had declined to

31 ± 8 and −21 ± 5 pA pF^{-1} at ± 60 mV, $n = 9$), whilst E_{rev} was unchanged (−8.6 ± 0.3 mV). Replacement of 100 mM bath NaCl by 100 mM sodium aspartate at this time gave a positive shift in E_{rev} of 15.1 ± 1.9 mV ($n = 4$). With increased $[Ca^{2+}]_i$, initial current densities in the Na^+-rich bath solution were elevated compared to 10 nM (124 ± 30 and −73 ± 17 pA pF^{-1} at ± 60 mV (300 nM) and 92 ± 26 and −60 ± 17 pA pF^{-1} at ± 60 mV (1000 nM)) with E_{rev} values of −5.1 ± 0.6 and −4.5 ± 0.8 mV, respectively ($n = 10$ for both data sets). In contrast to the decline in current densities seen at 10 nM Ca^{2+}, for elevated $[Ca^{2+}]_i$ mean current densities were maintained (at + 60 mV, 121 ± 66 and 93 ± 23 pA pF^{-1} for 300 and 1000 nM, respectively, $n = 10$). Replacement of bath NaCl by *N*-methyl-D-glucamine-Cl did not significantly alter current densities. Upon replacement of bath 100 mM *N*-methyl D-glucamine-Cl isosmotically by mannitol positive shifts in E_{rev} of 16.7 ± 1.5 mV ($n = 5$) and 17.6 ± 1.3 mV ($n = 7$), respectively, were observed.

Finally we investigated the behaviour of EGTA buffer capacity upon whole cell currents at a fixed $[Ca^{2+}]_i$ of 10 nM. Initial (1.5 min) current densities in a Na^+-rich bath were inversely correlated with EGTA concentration. At +60 mV these were, 91 ± 16, 76 ± 11 and 59 ± 3 pA pF^{-1} for 0.1, 2 and 5 mM EGTA, respectively ($n = 8$–11). Furthermore current density for 0.1 mM EGTA was elevated compared to 5.0 mM EGTA at 5 min (at +60 mV, 72 ± 28 and 31 ± 8 pA pF^{-1}, respectively).

The maintenance of whole-cell Cl^- currents at low (10 nM) buffered $[Ca^{2+}]_i$ but clear dependence upon EGTA buffer capacity suggests a model in which the Cl^- conductance is responsive to a raised local $[Ca^{2+}]$ possibly via a Ca^{2+} influx pathway at the apical plasma membrane of IMCD cells.

Stewart GS *et al.* (2001). *J Membr Biol* **180**, 49–64.

This work was supported by an NKRF studentship award to J.L.

All procedures accord with current UK legislation.

P48

Growth factor and cytokine regulation of glucose transport in equine articular chondrocytes

I. Ferraz*, T. Phillips†, S. Bell†, P.D. Clegg†, S.D Carter† and A. Mobasheri†

**Servicio de Reumatología, Hospital Universitario de Canarias, La Cuesta, 38320 La Laguna, Santa Cruz de Tenerife, Spain and †Faculty of Veterinary Science, University of Liverpool, Liverpool L69 7ZJ, UK*

Glucose serves as the major energy substrate for articular chondrocytes and the main precursor for the synthesis of extracellular matrix glycosaminoglycans in cartilage (Mobasheri *et al.* 2002*a*). Recent evidence suggests that articular chondrocytes express several facilitative glucose transporter (GLUT) isoforms (Mobasheri *et al.* 2002*b*) and also that 2-deoxyglucose transport is stimulated by cytokines (Shikhman *et al.* 2001). The aim of this investigation was to determine the effects of endocrine and cytokine factors on the capacity of equine articular chondrocytes for transporting 2-deoxyglucose and on the expression levels of GLUT1 and GLUT3.

Glucose transport into equine articular chondrocytes isolated using established procedures (from abattoir material) was determined by measuring the uptake of non-metabolizable 2-deoxy-D-[2,6-^{3}H]glucose in the presence and absence of glucose transport inhibitors (0.2 mM phloretin and 10 μM cytochalasin B) for a period 35 min at 20°C. Additional 2-deoxyglucose uptake experiments were performed with alginate encapsulated chondrocytes stimulated for 24 h with TNF-α (100 ng ml^{-1}), IL-1β (100 ng ml^{-1}), IGF-I (20 ng ml^{-1}) and TGF-β 20 ng ml^{-1}). Glucose uptake was normalized to total cell protein content using a Bio-Rad detergent-compatible (DC) protein assay. Western blotting was used to compare GLUT1 and GLUT3 expression levels of stimulated and unstimulated chondrocytes.

Results indicated that 2-deoxyglucose uptake was inhibited by up to 95% in the presence of cytochalasin B and/or phloretin, which suggests that glucose uptake into equine chondrocytes, is GLUT mediated. Treatment with IGF-I, TGF-β, IL-1β and TNF-α resulted in a significant increase (over 65%) in 2-deoxyglucose uptake compared to control values (Fig. 1). Short- and long-term administration of insulin (15 min and 24 h, respectively) did not increase glucose uptake ruling out a functional role for insulin-sensitive GLUT4-mediated glucose transport. GLUT1 and GLUT3 protein levels were found to be increased in chondrocytes stimulated with growth factors and cytokines.

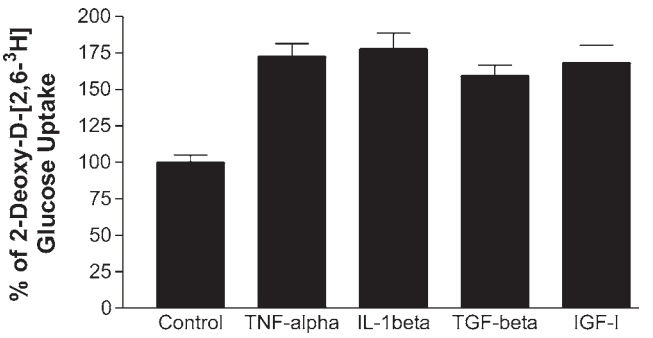

Figure 1. 2-Deoxy-D-[2,6-^{3}H]glucose uptake by equine articular chondrocytes stimulated with IGF-I, TGF-β, TNF-α and IL-1β. Baseline 2-deoxy-D-[2,6-^{3}H]glucose uptake in unstimulated chondrocytes (control) was considered as 100%. Error bars indicate standard errors of the means ($n = 3$).

The data presented support a critical role for glucose transport and metabolism in the synthesis and degradation of cartilage. Accelerated glucose transport via several GLUT isoforms represents a component of chondrocyte responses to both catabolic, pro-inflammatory cytokines and anabolic endocrine factors.

Mobasheri A *et al.* (2002*a*). *Histol Histopathol* **17**, 1239–1267.

Mobasheri A *et al.* (2002*b*). *Cell Biol Int* **26**, 297–300.

Shikhman AR *et al.* (2001). *J Immunol* **167**, 7001–7008.

We are grateful to the University Hospital of the Canaries and the Department of Pharmacology and Experimental Therapeutics, University of Liverpool for supporting this work.

All procedures accord with current UK legislation.

P49

Ion transport in distal lung epithelial cells isolated from adult and fetal rats

M.B. O'Shea, S.J. Ramminger, S.M. Wilson and R.E. Olver

Department of Maternal and Child Health Sciences, Ninewells Hospital and Medical School, University of Dundee, Dundee DD1 9SY, UK

Regulated transport of Na^+ is an important feature of the adult alveolar epithelial (ATII) cell and the mature fetal distal lung

epithelial (FDLE) cell. We compared the bioelectric properties of ATII cells and FDLE cells which have been cultured in conditions that favour the development of the adult cell phenotype.

ATII cells were isolated from rats killed by intraperitoneal injection of pentobarbital (10 mg (kg body weight)$^{-1}$) and FDLE cells were isolated from fetuses (gestational age 20 days) that were removed from anaesthetised rats (3 % halothane, killed before regaining consciousness). Cells were isolated by enzymatic digestion and incubated at adult alveolar P_{O_2} (100 mmHg) in minimally defined serum-free media and were treated with dexamethasone (200 nM) and tri-iodo-thyronine (T_3; 10 nM). FDLE and ATII cells formed resistive monolayers at 48 and 96 h, respectively, which were mounted in Ussing Chambers. At 96 h the mean baseline PD, I_{SC} and R_t of ATII and FDLE cells were 1.95 ± 0.29 mV, 6.62 ± 0.83 μA cm^{-2} and 337 ± 39 Ω cm^{-2} (n = 11) and 3.09 ± 0.83 mV cm^{-2}, 7.92 ± 0.35 μA cm^{-2} and 396 ± 110 Ω cm^{-2} (n = 4), respectively (mean ± S.E.M.; Student's paired t test). Addition of apical amiloride (10 μM) to both FDLE and ATII cells decreased basal I_{SC} by ~80 %, indicating predominantly sodium absorbing cells.

To establish the pharmacological properties of the ion channels underlying this Na^+ transport, concentration–effect curves were constructed for Na^+ channel antagonists. The rank order of potency amongst these compounds in both cell types was benzamil > amiloride > EIPA, suggesting that the highly selective epithelial Na^+ channel (ENaC) is involved in Na^+ transport across these cells.

We have previously (Collett *et al.* 2002) shown that addition of the β-adrenoceptor agonist isoprenaline to the basolateral membrane of FDLE cells at 48 h increases I_{SC} by ~60 % (n = 6, basal I_{SC}: 7.67 ± 0.63 μA cm^{-2}, peak increase I_{SC}: 12.07 ± 0.99 μA cm^{-2}, $P < 0.05$). This response is not evident when FDLE cells are maintained in culture for 96 h, basolateral isoprenaline induced no significant increase in I_{SC} (n = 4, basal I_{SC}: 8.76 ± 1.51 μA cm^{-2}, peak increase I_{SC}: 9.96 ± 1.25 μA cm^{-2} $P > 0.05$). In ATII cells stimulation with basolateral isoprenaline does not induce an increase in I_{SC}, but a significant decrease in I_{SC} (approximately 35%) was observed (n = 5, basal I_{SC}: 6.48 ± 0.52 μA cm^{-2}, peak decrease I_{SC}: 4.27 ± 0.39 μA cm^{-2}, $P < 0.05$). Further studies have shown that in ATII cells cultured in serum-containing media (DMEM: FBS (10%)) for the initial 48 h in culture, the observed decrease in I_{SC} in response to stimulation with isoprenaline is abolished (basal I_{SC}: 8.72 ± 0.98 μA cm^{-2}, peak increase I_{SC}: 9.59 ± 1.03 μA cm^{-2}, $P > 0.05$, n = 7).

Collett A *et al.* (2002). *Am J Physiol Lung Cell Mol Physiol* **282**, L624–L630.

All procedures accord with current UK legislation.

P50

Molecular sorting signals of the type II Na^+–P_i cotransporter family expressed in MDCK cells

C. Graham and A. Werner

School of Cell and Molecular Biosciences, University of Newcastle upon Tyne, Newcastle NE2 4HH, UK

Plasma phosphate levels are maintained by the type II sodium phosphate cotransporter family. NaPi-IIb mediates phosphate uptake from the small intestine followed by selective reabsorption from the renal proximal tubule by NaPi-IIa. It has previously been shown that expression of these cotransporters in MDCK cells results in differential sorting patterns. Mouse NaPi-IIa (mIIa) is expressed in both apical and basolateral membranes, whereas NaPi-IIb isoforms from flounder (fIIb) and mouse (mIIb) are preferentially sorted to the apical membrane (Hernando *et al.* 2000).

A ClustalW alignment of mIIa, mIIb and fIIb highlighted that the major differences between the type IIa and type IIb isoforms lie in the N- and C-termini as well as in the large extracellular loop (ECL3). We identified the C-terminus as the most likely candidiate for containing sorting information and so generated chimeras of these isoforms which allowed the C-termini to be switched. A schematic diagram of the generated chimeras used in this study is shown in Fig. 1.

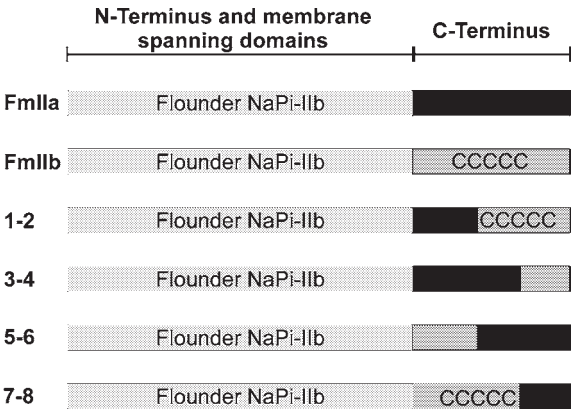

Figure 1. NaPi-II chimeras were generated with different C-termini.

MDCK cells grown on glass coverslips were transfected with the chimeras (Qiagen effectene), grown to confluency and fixed with 3 % paraformaldehyde. All chimeras contained an N-terminal EGFP tag, which allowed the recombinant proteins to be localised by confocal laser scanning microscopy.

As expected, exchanging the fIIb C-terminus with the same region from mIIb (chimera FmIIb) had no effect on the localisation. However, exchanging the C-terminus for that of mIIa (chimera FmIIa) led to a shift in the expression pattern to both apical and basolateral domains. Therefore, we concluded that the sorting signal lies within the C-terminus.

The C-termini of NaPi-IIb isoforms contain a stretch of cysteine residues that are absent in NaPi-IIa sequences. We investigated the role of this region in protein sorting by making four new chimeras of flounder NaPi-IIb with the C-terminus consisting of a combination of mIIa and mIIb (see Fig. 1).

Chimeras containing the cysteine-rich region from mIIb (1–2 and 7–8) were targeted to the apical membrane whereas chimeras lacking this region (3–4 and 5–6) were localised both in apical and basolateral membranes. These results strongly suggest an important role of the cysteine-rich region of the NaPi-IIb C-terminus for the correct targeting of this protein.

Hernando N *et al.* (2000). *Am J Physiol Renal Physiol* **278**, F361–F368.

All procedures accord with current UK legislation.

P51

Expression of facilitative glucose transporters in benign and metastatic human prostate cancer cell lines

N. Smith*, C.S. Foster† and A. Mobasheri*

Department of Veterinary Preclinical sciences, Faculty of Veterinary Science, University of Liverpool, Liverpool L69 7ZJ and †Department of Cellular and Molecular Pathology, Faculty of Medicine, University of Liverpool, Liverpool L69 3GA, UK

Cancer cells exhibit increased uptake and utilization of glucose in order to survive and continue their accelerated growth. Glucose uptake into mammalian cells is catalysed by members of the GLUT/SLC2A family of glucose/polyol transporters (Joost *et al.* 2002). Evidence suggests that facilitative glucose transporters (GLUTs) are implicated in the metabolic alteration of tumours (Burstein *et al.* 1998). Since the intermediary metabolism of prostate cells has been implicated in the pathogenesis of prostate adenocarcinoma and the progression from benign to malignant, metastatic prostate cancer (Costello & Franklin, 2000), we examined the expression of all the known members of the GLUT/SLC2A family in benign, weakly metastatic and strongly metastatic human prostate cancer cell lines.

Three prostate cell lines were used: an SV40 immortalized cell line derived from normal prostatic epithelial cells (PNT2) and two metastatic cell lines derived from prostatic carcinomas (DU145 and PC3). Cells were grown in RPMI 1640 supplemented with 2 mM L-glutamine, 10 % FCS, 100 μg ml^{-1} penicillin, 0.1 mg ml^{-1} streptomycin. Total RNA was isolated from each cell line and single stranded cDNA libraries constructed using Superscript II. Human specific oligonucleotide primers were designed to amplify PCR products corresponding to GLUTs 1–12 (except GLUT7) and the proton–myoinositol symporter HMIT1. β-Actin was also used as a positive control in all PCR experiments. PCR experiments were carried out at least three separate times for all known members of the GLUT/SLC2A family (repeated nine times for GLUT4 and GLUT9) for 35 cycles and the amplification products separated on 1 % agarose gels.

Transcripts of GLUT9 were not detected in the benign PNT2 cell line but were expressed in the metastatic DU145 and PC3 cell lines. GLUT5 was only detected in the PC3 cell line. All other GLUTs were detected in all cell lines examined except for GLUT4 which was detected in PC3 cells in three out of nine PCR experiments. HMIT1 was expressed in all three cell lines.

This study demonstrates, that strongly metastatic prostate cancer cell lines express additional GLUT isoforms not present in their benign counterparts (i.e. GLUT5 and GLUT9). This combination may confer the metastatic cells with a metabolic advantage that may encourage aberrant growth and promote metastasis.

Burstein DE *et al.* (1998). *Mod Pathol* **11**, 392–396.

Costello LC & Franklin RB (2000). *Oncology* **59**, 269–282.

Joost HG *et al.* (2002). *Am J Physiol Endocrinol Metab* **282**, E974–E976.

The University of Liverpool Research Development Fund supported this study.

P52

Developmental expression of the GLUT9 facilitative glucose transporter in ovine articular cartilage

A. Mobasheri*, S.D. Carter*, J.F. Innes*, S. Richardson*, J.F. Moley† and K.H. Moley‡

Faculty of Veterinary Science, University of Liverpool, Liverpool L69 7ZJ, UK and Departments of †Surgery, ‡Obstetrics, Gynecology, Cell Biology and Physiology, Washington University School of Medicine, St Louis, MO 63110, USA

The transport of glucose and glucose-derived compounds across the chondrocyte membrane is essential for chondrogenesis and the development of the skeletal system. Chondrocytes express multiple isoforms of the GLUT/SLC2A family of glucose transporters (Ohara *et al.* 2001; Shikhman *et al.* 2001; Mobasheri *et al.* 2002) including the recently identified GLUT9 (SLC2A9; Phay *et al.* 2000). This study reports the expression and localization of GLUT9 in ovine cartilage from various developmental stages.

Ovine embryos were obtained from killed pregnant ewes. All procedures were carried out strictly in accordance with current UK legislation. Animals were humanely killed by injection with 0.75 ml (kg body weight)$^{-1}$ sodium pentobarbitone (Euthatal, Rhône Mérieux, 200 mg ml^{-1}). Full-depth cartilage plugs were excised from the forelimbs of newborn and 2-year-old animals (abattoir material) using a cork borer. All tissues (including forelimbs of embryos) were fixed in neutral buffered formalin before decalcification in 10 % EDTA and immunohistochemistry. Antigen retrieval was performed in the microwave oven in the presence of 10 mM citrate buffer (pH 6.0) and endogenous alkaline phosphatase quenched by treatment with 1.25 mM levamisole. Non-specific protein binding sites were blocked by incubation with 10 % normal goat serum in phosphate buffered saline (PBS). Sections were probed with primary polyclonal antibodies to mouse GLUT9 and secondary goat anti-mouse IgG conjugated to alkaline phosphatase. Alkaline phosphatase active sites were revealed using Fast-Red TR/Naphthol AS-MX as precipitating agent. Sections were counterstained with haematoxylin and mounted in aqueous medium before examination by light microscopy.

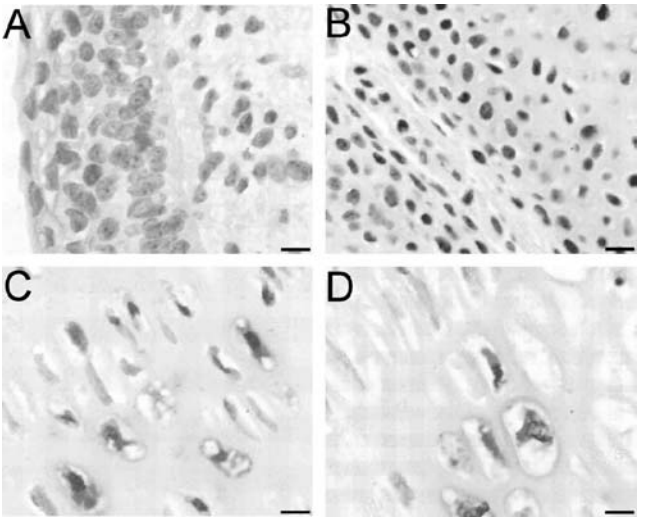

Figure 1. Immunohistochemical localization of GLUT9 in forelimbs of sheep embryos. GLUT9 staining was observed in articular chondrocytes (*B*) and epiphyseal chondrocytes (*C* and *D*) but was absent in hoof dermal keratinocytes (*A*). Scale bars, 10 μm.

The results revealed that GLUT9 is abundantly expressed in developing chondroblasts and chondrocytes in ovine embryos (Fig. 1) and in the superficial, middle and deep layers of developing ovine cartilage. Closer examination revealed that GLUT9 is present in an intracellular, perinuclear location in fetal, developing and adult chondrocytes. GLUT9 was also found in an intracellular location in the kidney, ileum and placenta. Articular cartilage is a poorly vascularized and highly glycolytic tissue that produces large quantities of lactic acid. This situation is further exacerbated by low oxygen tensions and ongoing anaerobic glycolysis by chondrocytes. Expression of multiple GLUT isoforms including GLUT1, GLUT3, GLUT4, GLUT9 and GLUT12 may be an important physiological and bioenergetic adaptation for chondrocytes in the extracellular matrix in developing cartilage (Macheda *et al.* 2002).

Macheda ML *et al.* (2002). *Anat Embryol* **205**, 441–452.
Mobasheri A *et al.* (2002). *Cell Biol Int* **26**, 297–300.
Ohara H *et al.* (2001). *Acta Histochem* **103**, 365–378.
Phay JE *et al.* (2000). *Genomics* **66**, 217–220.
Shikhman AR *et al.* (2001). *J Immunol* **167**, 7001–7008.

All procedures accord with current UK legislation.

P54

Differential effects of nucleotides upon ion transport in H441 human bronchial epithelial cells

S.J. Ramminger, M.T. Clunes, R.E. Olver and S.M. Wilson

Lung Membrane Transport Group, Tayside Institute of Child Health, Department of Maternal and Child Health Sciences, Ninewells Hospital and Medical School, University of Dundee, Dundee DD1 9SY, UK

Apical nucleotides inhibit Na^+ transport in many absorptive epithelia and these responses are often attributed to apical receptors belonging to the $P2Y_2$ subclass, which characteristically display equally sensitive to ATP and UTP (see e.g. Ramminger *et al.* 1999). In the present study we have explored the effects of apical nucleotides upon Na^+ transport in dexamethasone-treated (0.2 μM) H441 human bronchial epithelial cells as this cell line has recently been shown to generate amiloride-sensitive I_{SC} after treatment with this synthetic glucocorticoid (Sayegh *et al.* 1999). Our data show that ATP elicited a complex response (Fig. 1A) which initially consisted of an increase in I_{SC}. However, this was succeeded by a slowly developing fall in I_{SC} until, after ~30 min exposure to this nucleotide, I_{SC} had fallen below its initial control value ($P < 0.05$, Student's paired t test). The response to UTP (Fig. 1*B*), in contrast, consisted of an initial brief transient followed by a rapid and persistent fall ($P < 0.002$) in I_{SC}. These two nucleotides thus have markedly different effects, a finding which is inconsistent with the view that these nucleotides act via a common receptor population. ADP, a nucleotide that does not activate $P2Y_2$ receptors but which is an agonist at certain other P2Y receptor subtypes, including $P2Y_1$ receptors, evoked a monophasic increase in I_{SC} (Fig. 1*C*). H441 cells thus express a complex population of apical P2Y receptors which allow both stimulatory and inhibitory control over amiloride-sensitive I_{SC}. The differential effects of ATP and UTP is similar to the situation in the isolated porcine trachea, where UTP, but not ATP, can exert inhibitory control over Na^+ absorption (Inglis *et al.* 2000).

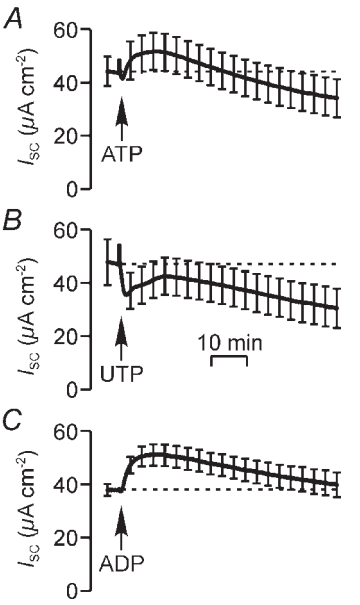

Figure 1. Effects of nucleotides upon I_{SC}. H441 cells were grown on permeable supports in serum-free medium supplemented with dexamethasone (0.2 μM) where they formed resistive monolayers within 7–10 days. These cultured epithelia were mounted in Ussing chambers to allow the effects of apical nucleotides upon the spontaneous current to be explored. *A–C,* the responses to 100 μM apical ATP ($n = 7$), UTP ($n = 4$) or ADP ($n = 6$), respectively (means ± S.E.M.).

Inglis SK *et al.* (2000). *Br J Pharmacol* **130**, 367–374.
Ramminger SJ *et al.* (1999). *Br J Pharmacol* **128**, 293–300.
Sayegh R *et al.* (1999). *J Biol Chem* **274**, 12431–12437.

This work was supported by the Wellcome Trust and Tenovus (Scotland).